SLAC–PUB–4797 Rev.
February 1989
(T)

Cross Sections for Lepton– and Baryon–Number Violating Processes From Supersymmetry at $P - \bar{P}$ Colliders*

SAVAS DIMOPOULOS

Department of Physics
Stanford University, Stanford, California 94305

RAHIM ESMAILZADEH

Stanford Linear Accelerator Center
Stanford University, Stanford, California 94309

LAWRENCE J. HALL

Department of Physics
University of California, Berkeley, California 94720

JEAN-PIERRE MERLO

CERN, CH–1211, Geneva 23 Switzerland

GLENN D. STARKMAN

Institute for Advanced Study
Princeton, New Jersey 08540

Submitted to *Physical Review D.*

* Work supported by the Department of Energy, contract DE–AC03–76SF00515.

ABSTRACT

In the standard minimal low-energy supersymmetric model, superpartners are produced only in pairs and the lightest superpartner is stable. At hadron colliders missing transverse energy is the most important signature for this model. There are two other minimal supersymmetric models; one has lepton-number violation, the other baryon-number violation. In both models superpartners can be singly produced and the lightest superpartner is unstable. At hadron colliders missing transverse energy is a poor signature for these models. However, there are several important signatures. The most spectacular signatures have two or more isolated charged leptons occurring typically in events with jets. Superpartner masses may be reconstructed from combinations of lepton-jet invariant masses and from jet spectroscopy. Cross sections are presented for the most important single and pair superparticle production mechanisms in $p-\bar{p}$ collisions. Present limits from CERN collider data are given and a variety of signatures, events and backgrounds at $\sqrt{s} = 2$ TeV are discussed. For example, Drell Yan fusion of a single superpartner gives a bump in the two-jet invariant mass cross section at the superpartner mass. Squark pair production could yield events with two jets and two isolated charged leptons. If the lightest superpartner is long lived, it can give rise to secondary vertices or to signatures in stable particle searches. A run of $10pb^{-1}$ at $\sqrt{s} = 2$ TeV will enable a large region of the parameter space to be explored.

1. INTRODUCTION

Supersymmetry is currently an elegant mathematical theory desperately in need of experimental evidence. The majority of accelerator searches for supersymmetry assume that the lightest superpartner (LSP) is stable, and has neither strong nor electromagnetic interactions.[1] Therefore, the trademark for supersymmetry has been missing energy. Although such an LSP can arise in some minimal* supersymmetric models, such models are constrained to have the fewest Yukawa-type interactions consistent with the known fermion masses. This constraint is nontrivial and it excludes those gauge invariant interactions which allow the LSP to decay. More general models have lepton- or baryon-numbers violating Yukawa interactions and predict completely different accelerator signatures. For example, they predict single superparticle production and leptonic signatures in hadron colliders.

In a previous paper,[2] Dimopoulos and Hall discussed various possible models, experimental tests and limits on the strength of these Yukawa couplings. The reader is urged to review Ref. 2, especially for a discussion of the three minimal supersymmetry models. In this paper we present the cross sections for production of supersymmetric particles in $p - \bar{p}$ colliders, arising in supersymmetric theories with lepton- or baryon-number violating Yukawa interactions at the weak scale.

The standard minimal low energy supergravity theory results when R parity or matter parity is imposed on the couplings. This constraint removes renormalizable baryon and lepton number violating interactions. If baryon number is imposed, the couplings

$$q\bar{d}\ell, \ell\ell\bar{e} \qquad\qquad \Delta L \neq 0 \tag{1.1}$$

are allowed, giving a model which violates lepton number, the "$\Delta L \neq 0$" model.

---

* We call a supersymmetric model minimal if it has the fewest number of particles possible. These include particles of the standard model, an extra Higgs doublet and all the superpartners.

If lepton number is imposed, the coupling

$$\bar{u}\bar{d}\bar{d} \qquad\qquad \Delta B \neq 0 \tag{1.2}$$

is allowed, giving a model which violates baryon number, the "$\Delta B \neq 0$" model.[2] Some vertices resulting from Eqs. (1.1) and (1.2) are drawn in Fig. 1. The flavor structure of the new interactions can be very rich. For our purposes, we will generally assume that the operator which gives the largest signal and does not violate any other laboratory results, dominates. In most cases, the coupling constant for the dominant operator can be of order 1. In the last section we shall discuss possible exotic signatures if this is not the case, and also discuss some limits from existing data.

We shall organize our work by the possible production channels: we will first discuss single supersymmetric-particle production and then mention pair production of gluinos, squarks and sleptons. In each case we shall present the dominant interactions, the production cross section, the experimental signature and the background. The general framework of our analysis is the same as Refs. (3) and (4); we integrate over the elementary tree level production cross sections and the parton distribution functions of Ref. (3). For the distribution functions we use set two of Ref. (3) where the QCD parameter is set equal to 0.29 GeV. The reader who is not interested in the formulae for the cross sections should only review the figures and then go directly to Section 4 where we discuss some limits from existing data, prospects for detecting superpartners in the near future and some exotic decays of the LSP.

It is worth mentioning that there are a host of other experimental predictions of such models. There have already been studies of rare processes: K, π, ν decays, ν masses and oscillations,[5–10] neutron oscillation and heavy nucleus decays.[11,12] Other possibilities include signatures in e^+e^- machines, rare Z decays or B decays. Dimopulos and Hall have also proposed that such baryon number violating models are responsible for a low-energy (10 MeV) era of baryogenesis, which could account for the baryon asymmetry of the universe.[13]

2. SINGLE SUPERPARTICLE PRODUCTION

The sneutrino resonance production occurs in hadron colliders ($d\bar{d} \to \tilde{\nu}$) (Fig. 2) through the lepton-number violating operator $\bar{q}d\ell$. We shall assume that the dominant decay is the reverse of the production mechanism, and hence, the signature for $\tilde{\nu}$ is a bump in invariant mass for the two-jet cross section. Then the elementary cross section is given by Ref. (14):

$$\sigma(d\bar{d} \to \tilde{\nu}) = \frac{1}{3} \frac{\frac{4\pi}{3}\Gamma^2}{(\hat{s} - m^2)^2 + m^2\Gamma^2} \tag{2.1}$$

where Γ is the width of $\tilde{\nu}$ and is given by

$$\Gamma(\tilde{\nu} \to d\bar{d}) = \frac{3\alpha_\lambda}{4} m \quad ; \tag{2.2}$$

m is the mass of $\tilde{\nu}$, $\hat{s}$ is the square of the parton c.m. energy and $\alpha_\lambda = \lambda^2/4\pi$. The factor of $1/3$ in front is from matching the initial colors.

To compute the interaction rate we follow the usual formalism of the parton model of hadrons (for more detail see Ref. (3)). The cross section for any hadronic reaction

$$a + b \to c + anything \tag{2.3}$$

is given by

$$d\sigma(a + b \to c + X) = \sum_{i,j partons} f_i^{(a)} f_j^{(b)} d\hat{\sigma}(i + j \to c + X') \tag{2.4}$$

where $f_i^{(a)}$ is the probability of finding parton i in hadron a, and $\hat{\sigma}$ is the cross section for the elementary process resulting in the desired final state. The parton distributions are measured experimentally at a given scale, and then they are evolved to the very large momentum scales of interest via the Altarelli-Parisi equations. They are generally functions of the Bjorken scaling variable x and Q^2, the square of the characteristic energy scale of the process under consideration.

A very useful quantity is the differential parton-parton luminosity

$$\tau\frac{d\mathcal{L}}{d\tau} \equiv \frac{\tau}{1+\delta_{ij}}\int_{\tau}^{1} dx[f_i^{(a)}(x)f_j^{(b)}(\tau/x) + f_j^{(a)}(x)f_i^{(b)}(\tau/x)]/x \quad , \tag{2.5}$$

where τ is given by

$$\tau = \hat{s}/s \quad , \tag{2.6}$$

and $\sqrt{s}$ is the c.m. energy of the colliding hadrons. The differential luminosity is the number of parton collisions with c.m. energies between τ and $\tau + d\tau$ per hadron collision. Therefore, the cross section for the hadronic reaction (Eq. (2.3)) is given by

$$\frac{d\sigma}{d\tau}(ab \to cX) = \sum_{ij} \frac{d\mathcal{L}_{ij}}{d\tau}\hat{\sigma}(ij \to c) \quad , \tag{2.7}$$

where $\hat{\sigma}$ is the cross section for the elementary process.

Usually, one must integrate over τ, hence effectively integrating over all parton-parton c.m. energies, to compute the total hadronic cross section. In the case of resonance production of a particle, such as the $\tilde{\nu}$, we can make a further approximation. In the narrow resonance limit all the contribution to $p\bar{p} \to \tilde{\nu} + X$ essentially comes from the parton c.m. energies equal to the mass of $\tilde{\nu}$. Therefore we can replace the expression for the cross section by:

$$\hat{\sigma} = \frac{4\pi^2}{9}\frac{\Gamma}{m}\delta(\hat{s} - m^2) \tag{2.8}$$

where now $\hat{\sigma}$ is the parton cross section, and $\sqrt{\hat{s}}$ is the parton c.m. energy. This δ-function removes the integral over τ and finally we get

$$\sigma(p\bar{p} \to \tilde{\nu}X) = \frac{4\pi^2}{9}\frac{\Gamma}{m} \times (\frac{\tau}{\hat{s}}\frac{d\mathcal{L}}{d\tau})|_{\tau=m^2/s} \quad , \tag{2.9}$$

where $\frac{d\mathcal{L}}{d\tau}$ represents the differential $d\bar{d}$ luminosity in $p\bar{p}$ collisions evaluated at the mass of $\tilde{\nu}$. Figure 3 shows the values of $\frac{\tau}{\hat{s}}\frac{d\mathcal{L}}{d\tau}$ as a function of $\sqrt{\hat{s}}$ in $p - \bar{p}$ collisions

for various collider energies $\sqrt{s}$. Now, using this graph it is easy to read off the cross section for $\tilde{\nu}$ production in $p-\bar{p}$ collisions. In Fig. 4, we present the total cross section for $p\bar{p} \to \tilde{\nu}$ as a function of the collider c.m. energy, for various $\tilde{\nu}$ masses, with $\lambda = 1$. The result is proportional to λ^2.

At Fermilab Tevatron collider energies, $\sqrt{s} = 2000$ GeV, the cross section for producing 100 GeV $\tilde{\nu}$'s is about 8 nb; with an average luminosity of 10^{30} cm^{-2} sec^{-1}, an experiment running for 10^7 sec could accumulate 8×10^4 events.

Next, there is the resonance production of $\tilde{\ell}^{\pm}$ through the operator $\bar{q}dl$. With essentially the same assumptions as for the $\tilde{\nu}$, and the same analysis, we shall proceed to present the results. In Fig. 5, we show the parton luminosity resulting to $\tilde{\ell}^{\pm}$ production. The $\tilde{\ell}^{\pm}$ are produced by the elementary reactions $u\bar{d} \to l^+$ and $\bar{u}d \to l^-$ (Fig. 2). In Fig. 6, we present the total production cross section for $\tilde{\ell}^{\pm}$ production in $p-\bar{p}$ colliders for various collider energies.

The presence of a baryon-number violating Yukawa coupling ($\bar{u}\bar{d}\bar{d}$) can result in the production of single squarks (Fig. 7) which can decay into two quarks and produce two jets with an invariant mass equal to the mass of the squark. The analysis is again similar to the $\tilde{\nu}$ and $\tilde{\ell}^{\pm}$; the formula Eq. (2.9) also applies to $\tilde{q}$ production except for an extra factor of two from mismatch of initial color states, so that $4 \to 8$. Also, $\frac{d\mathcal{L}}{d\tau}$ now refers to a ud not a $d\bar{d}$ luminosity. Here we assumed the dominant operator has the flavor structure $u\bar{d}\bar{b}$, so the superpartner is a b flavor squark. The $\bar{u}\bar{d}\bar{s}$ operator would give us similar results, except the coefficient of this operator must be necessarily small ($\leq 10^{-6}$), from neutron oscillations and nucleus decay. We present the results in Figs. 8 and 9.

As we emphasized before, the $\tilde{\nu}$, $\tilde{\ell}^{\pm}$ and $\tilde{q}^{\pm 1/3}$ decay into a $q-q$ pair, producing two jets. Therefore, the signature for the presence of these superpartners is a bump in the two-jet invariant mass plot. The production cross sections for $\tilde{\ell}$ and $\tilde{q}$ for $\lambda = 1$ are larger than $W^{\pm}$ and Z^o for comparable masses, and since hadronic decays of these particles have been seen by UA2, we suggest that it is possible to either detect the signature for the superpartners, or set limits on the masses and

the strength of the baryon- and lepton-number violating Yukawa couplings (more on this in the last section). It also is possible for the main decay modes to be $\tilde{\nu} \to \nu\tilde{Z}$ and $\tilde{\ell}^{\pm} \to \ell^{\pm}\tilde{\gamma}$ where the light neutralino, a $\tilde{\gamma}$ or a $\tilde{Z}$, then decays to $\bar{q}q\ell$. This then gives either missing transverse energy or a hard lepton recoiling against jets and a lepton. This is perhaps a better signature than a bump in the two-jet invariant mass plot.

In the baryon-number violating models, single gluinos can be produced via two quarks exchanging a squark in the t or u channels (Fig. 10). As we mentioned before, $\bar{u}\bar{d}\bar{d}$ couplings are constrained to be small ($\leq 10^{-6}$) for the lowest generation structure ($\bar{u}\bar{d}\bar{s}$) from neutron oscillations and nucleus decay. Let's consider the case where the dominant $\bar{u}\bar{d}\bar{d}$ operator has a higher generation structure, such as $\bar{u}\bar{d}\bar{b}$. Defining the convenient quantities

$$\xi = [s - (m_1 + m_2)^2]^{1/2}[s - (m_1 - m_2)^2]^{1/2} \tag{2.10}$$

$$\Delta_{ai} = M_a^2 - m_i^2 \quad , \tag{2.11}$$

$$\Lambda_a = ln[\frac{s + \Delta_{a1} + \Delta_{a2} - \xi}{s + \Delta_{a1} + \Delta_{a2} + \xi}] \quad , \tag{2.12}$$

the elementary cross section for single gluino production is

$$\begin{aligned} \sigma(ud \to \tilde{g}\bar{b}) = & \frac{16\alpha_s\alpha_\lambda}{9} \\ & [\{(\xi + (\Delta_{t1} + \Delta_{t2})\Lambda_t + \frac{\xi\Delta_{t1}\Delta_{t2}}{M_t^4 + m_1^2m_2^2 + M_t^2(s - m_1^2 - m_2^2)}) + (t \leftrightarrow u)], \\ & + \frac{2m_1m_2s}{(s + \Delta_{t1} + \Delta_{u2})}(\Lambda_t + \Lambda_u)\} \end{aligned} \tag{2.13}$$

where α_s is the strong coupling constant, $\alpha_\lambda = \lambda^2/4\pi$, and m_1 and m_2 are the masses of the outgoing particles, the b-quark and the gluino, and M_t is the mass of the t-channel exchanged particle, the squark, etc.

In $p-\bar{p}$ collisions, single gluinos are produced by the elementary reactions $ud \rightarrow \tilde{g}\bar{b}$ and $\bar{u}\bar{d} \rightarrow \tilde{g}b$. If $\lambda \gtrsim 1$ so the production is large, then the gluino predominantly decays into three quarks. Hence the signature for single $\tilde{g}$ production is four possibly coalesced jets. In Fig. 11, we present the cross section for $p\bar{p} \rightarrow \tilde{g}+q$ *or* $\bar{q}$, which was computed by integrating the elementary cross section (Eq. (2.13)) over the appropriate parton distribution functions. Gluino single production compared to squark single production could be more important since the four-jet background for detecting gluinos is much smaller than the two-jet background for detecting squarks. Also, the gluino could be much lighter than the squark and therefore more abundantly produced.

It is also possible that in the "$\Delta B \neq 0$" model, the operator that dominates is $\bar{c}\bar{b}\bar{s}$, in which case the decays $\tilde{g} \rightarrow qqq$ will contain several $K, D, B...$ mesons and frequently a Λ (Fig. 12). In Fig. 13, we present the total cross section for $p\bar{p} \rightarrow \tilde{g}q$ if the dominant operator is $\bar{c}\bar{b}\bar{s}$.

This concludes our discussion of single superpartner particle productions in $p-\bar{p}$ collisions. To summarize, sleptons and squarks decay into quarks producing two jets, where the signature is a bump in the two-jet invariant mass plot. The gluino can decay into three quarks, producing up to four jets in the final state, some of which might contain a high number of higher generation mesons and baryons.

3. SUPERPARTICLE PAIR PRODUCTION

The cross section for gluino pair production in $p-\bar{p}$ colliders has been computed in Ref. (4). It occurs via the usual gauge couplings present in the minimal supersymmetric version of the standard model. Figure 14 presents the total cross section for gluino pair production. In the "$\Delta B \neq 0$" models, the gluino decays into at least three quarks, producing multi-jet event. For the models with the $q\bar{d}\ell$ operator, each gluino can decay into a quark and an antiquark and a charged or neutral lepton. The signature would be up to four jets and up to two isolated charged leptons with possible missing energy. If the photino is lighter than the

gluino and the squark, the gluino can decay via $q\bar{q}\tilde{\gamma}$ to give a total of eight quarks and two leptons of any charge. The signature would be similar, except the leptons would be softer and the events more spherical. If the $\ell\ell\bar{e}$ operators are present, then the photino would decay into three leptons and the final state would consist of up to four jets, four charged leptons and possible missing energy. A run at the Fermilab Tevatron with luminosity of $1pb^{-1}$ should easily exclude or find a gluino lighter than 100 GeV in this model.

Slepton pair production can occur in the presence of the $q\bar{d}\ell$ operator, via the elementary processes $d\bar{d} \to \tilde{\ell}\tilde{\ell}^*$ and $u\bar{u} \to \tilde{\ell}\tilde{\ell}^*$. The cross section is given by

$$\sigma(q_i\bar{q}_i \to \tilde{\ell}\tilde{\ell}^*) = \frac{2\pi\alpha_\lambda^2}{3}\left(\frac{s-2m^2}{s^2}\right)\left(log\left(\frac{1+b}{1-b}\right) - 2b\right) \quad , \tag{3.1}$$

where

$$b = \frac{\sqrt{s(s-4m^2)}}{s-2m^2} \quad .$$

The total cross section for $p\bar{p} \to \tilde{\ell}\tilde{\ell}^*$ is shown in Fig. 15, for $\lambda = 1$. The sleptons then decay into two quarks each, resulting in up to four jets in the final state.

Squark pair production via the usual gauge couplings has been computed (Eq. (4)). In Fig. 16, we present the total cross section for pair production of squarks. In the presence of the lepton-number violating operators, a squark can decay into a quark and a charged or neutral lepton, producing two jets and two charged leptons or missing energy in the final state.

Squarks can also be produced via the presence of the $\bar{u}\bar{d}\bar{d}$ operator, i.e., $u\bar{u}$ or $d\bar{d}$ going into a $\tilde{b}\tilde{b}^*$ pair. In Fig. 17, we present the contribution to the cross section for $p\bar{p} \to q\tilde{q}^*$ coming from the square of the matrix element due to the $\bar{u}\bar{d}\bar{d}$ operator. In this scenario, a squark decays into two quarks, thereby giving up to four jets in the final state.

To summarize, the $\Delta B \neq 0$ model gives multi-jet events with two or three jets with invariant mass equal to the squark or gluino mass. The characteristic signature of the $\Delta L \neq 0$ models is events with isolated charged leptons.

4. EXISTING LIMITS, FUTURE PROSPECTS AND EXOTIC SIGNATURES

In this section we shall present some limits on the superpartner masses and the strength of the Yukawa operators coming from the data already published. We also shall discuss the prospects for detection of singly produced superpartners in a 2 TeV machine, e.g., the Fermilab Tevatron. In the final subsection, we shall enumerate the LSP decays in the presence of the B- and L-number violating operators, and discuss what happens if the couplings for these operators are small ($\lambda \sim 10^{-8}$) and therefore the LSP is relatively long lived.

4.1. Limits From the CERN Collider

It already is possible to set some very modest limits on the masses and the Yukawa couplings of the superpartners using the existing data from the CERN $p - \bar{p}$ collider.

Limits From UA1

In a recent paper,[15] upper limits are set on the cross section times the decay branching ratio for the production of any particle (a vector or a scalar) decaying into two hadronic jets. The limits are for a particle X with a width $\Gamma_X < 0.4 M_X$, as a function of mass M_X for $M_X > 150$ GeV (Fig. 18). The data is from the CERN collider with the center of mass energy $\sqrt{s} = 630$ GeV. We also have shown in Fig. 18, the cross sections for sneutrino, squark and slepton production as a function of the mass for the same center of mass energy, for $\lambda = 2.2$ corresponding to Γ of $0.4m$, assuming a branching ratio of one into two jets. The predicted cross sections only lie in the excluded region for restricted masses and couplings for the single slepton production.

Limits From UA2

Limits for smaller masses can be obtained from the published results of the UA2 collaboration. In Ref. (16), the invariant mass distribution of jet pairs is examined in the search for decays of the $W^{\pm}$ and Z^o bosons into quark–antiquark pairs. The UA2 results are shown in Fig. 19. Unfortunately, this data has not been converted into a limit on other scalar or vector particles decaying into two jets. To derive such a limit, one is required to carry on a Monte Carlo simulation of production and decay of X particle in the UA2 detector. Such a simulation must take into account the experimental efficiency and the geometrical acceptance of the detector, and also include all the experimental cuts for identifying the final jets and their invariant mass. While we encourage the UA2 collaboration to carry on this program, we have derived certain limits without the use of a Monte Carlo program, based on the following procedure.

We assume that the efficiency of the detector to detect two-jet decays of X, i.e. the percentage of the two-jet events that are detected and pass all the experimental cuts, is independent of the mass of X and equivalent to that of the $W^{\pm}$ and Z^o. To estimate this quantity, we first compute the number of jet pairs coming from the decays of these intermediate vector bosons (IVB). The total integrated luminosity associated with the UA2 data is $L_t = 0.73bp^{-1}$. The total cross section for W production is predicted to be $\sigma_W(630\text{GeV}) = 5.8nb$, and for Z production $\sigma_Z(630\text{GeV}) = 1.7nb$ (Ref. (17)). We also estimate the branching ratios $B(W \to qq) = 0.6$ and $B(Z \to qq) = 0.9$. Therefore, the expected number of two jets coming from the IVB decays is $730nb^{-1} \times (5.8nb \times 0.6 + 1.7nb \times 0.9) \simeq 3.7 \times 10^3$. The UA2 collaboration using a detailed Monte Carlo program predicts a total number of 340 ± 80 two-jet events. Hence, the ratio of number of two-jet events detected to the number of produced IVB's decaying into two jets is about $\frac{340 \pm 80}{3.7 \times 10^3} \simeq 9 \pm 2\%$. We shall take this ratio to be 7%, since this will give us the most confident bounds.

We also assume that a structure at the level of $\simeq 5$ standard deviations over the background is ruled out by the data. Consequently, we derive a limit on

the production cross section times the branching ratio into quark–antiquark pairs, which is presented in Fig. 20. These limits match the UA1 reported limits in the mass region where the two data sets overlap. This makes us more confident that the limits we derived are similar to the true limits that are obtained by running a Monte Carlo simulation.

The broken lines in Fig. 20 show the production cross sections for sleptons, squarks and sneutrinos with $B = 1$ and $\lambda = 1.3$ corresponding to a width of $\Gamma = 0.1M$. We restricted the analysis to X particle with width $\Gamma_x < 0.1m_x$, since the best mass resolution achieved is about 10%. A particle with a larger width is harder to rule out because it produces a wider resonance which can be difficult to separate from the background. We do believe that some larger λ's are ruled out; however, we leave the definite bounds to the detailed Monte Carlo simulation. In Fig. 21, the dark region in the m_x vs. λ plane is excluded by the existing data. Obviously, experiments are just beginning to explore this domain. Tevatron data will allow a search for these particles over a wider range of parameters.

4.2. Prospects for Detecting Superpartner Production at the Fermilab Tevatron

a) Single Superparticle Production — Two-Jet Decays

We already have mentioned that if the dominant mechanism for $\tilde{\nu}, \tilde{\ell}$ and $\tilde{q}$ decay is into two quarks forming two jets, the signature is a bump in the two-jet invariant mass plot. Let us discuss the possibility of seeing this signal in a 2 TeV machine. The invariant mass spectrum for two-jet events produced in $p - \bar{p}$ collisions has been computed in Ref. (3), and is presented in Fig. 22 for collision energy $\sqrt{s} = 2$ TeV. This jet–jet mass spectrum represents the background for any of the superparticles which decay into two jets. The signal has a peak with a height $\propto 1/m^2$ which is independent of λ, and a width $\propto \lambda^2 m$. For example, in the case of $\tilde{\nu}$ production, the height of the signal in the two-jet invariant mass spectrum is

equal to

$$\frac{d\sigma}{dM}|_{peak} = \frac{8\pi}{9}\frac{1}{m} \times (\frac{\tau}{\hat{s}}\frac{d\mathcal{L}}{d\tau})|_{\tau=m^2/s} \quad , \tag{4.1}$$

where $(\frac{\tau}{\hat{s}}\frac{d\mathcal{L}}{d\tau})$ is the parton–parton luminosity depicted in Fig. 3; M, the invariant mass of two jets is a variable; and m is the mass of the $\tilde{\nu}$. For comparison, we have plotted this function on Fig. 22 (dashed line). The signal is about an order of magnitude smaller than the background for all $\tilde{\nu}$ masses. The situation is very similar to the decays of $W^{\pm}$ and Z^o into quark–antiquark pairs, where such a signature has been observed by the UA2 collaboration (Ref. (16)). To get an idea of what sort of total luminosity is needed to "discover" the sneutrinos, let's assume the following criterion: if the signal is five times the statistical error in the background, then this could constitute a positive signature. Let's assume that the best jet energy resolution that can be achieved is about 10% of the total jet energy. We also assume that the width of the $\tilde{\nu}$ resonance is smaller than this resolution, i.e. $\Gamma_{\tilde{\nu}} < 0.1M_{\tilde{\nu}}$. If N is the number of $\tilde{\nu}$'s produced, and B is the number of events in the background in a bin of size $0.1M_{\tilde{\nu}}$ around the sneutrino mass, then we require as our "discovery criterion" that $\frac{N}{\sqrt{B}} = 5$. The number of events in the background is given by

$$B = 0.1 \times M_{\tilde{\nu}} \times \frac{d\sigma}{dM}|_{jet-jet} \times L_t \quad , \tag{4.2}$$

where L_t is the total integrated luminosity. The number of $\tilde{\nu}$'s produced with the same total luminosity is given as

$$N = \frac{\Gamma_{\tilde{\nu}}}{2}\frac{d\sigma}{dM}|_{peak} \times L_t \quad . \tag{4.3}$$

Again assuming that the QCD background is about an order of magnitude larger than the peak of the $\tilde{\nu}$ resonance, we can solve for the minimum total luminosity required to satisfy our "discovery" criterion:

$$L_t = 0.5pb^{-1} \times (\frac{0.1M_{\tilde{\nu}}}{\Gamma_{\tilde{\nu}}}) \times (\frac{nb}{\sigma_{\tilde{\nu}}}) \quad . \tag{4.4}$$

Figure 23 shows the integrated luminosity necessary to satisfy our condition for

collider energy of 2 TeV, assuming $\lambda = 1$. We must stress that these numbers are just simple estimates and we encourage future Monte Carlo simulations to take care accurately of a detector's geometry and design specifications.

From Eq. (4.4), we know that L_t scales as $\frac{1}{\lambda^4}$ since both the width and the production cross section are proportional to α_λ. This rule with Fig. 23 allows one to estimate the luminosity needed for any mass and coupling. If λ is less than 0.1, it is unlikely that single superparticle production would be detected as a resonant bump in the two-jet mass spectrum. However, one could look for other decay modes of a singly produced superparticle which are not drowned by a large QCD background. Such decays include prominent leptonic decays and three-jet decays of a singly produced gluino, which we shall discuss in the next two subsections.

Three-Jet Decays

We already have presented the cross sections for single production of gluinos in the presence of the $\bar{u}\bar{d}\bar{d}$ operator; the final state contains four jets, three of which come from the decay of the gluino and therefore have the invariant mass equal to the gluino mass. The four-jet QCD background, for $\sqrt{s} = 2$ TeV, is estimated to be about $10nb$ (Ref. (18)), where each jet energy must be more than 15 GeV and the sum of all the jet energies must be greater than 70 GeV. The gluino production cross section is $4nb$ for $m_{\tilde{g}} = 50$ GeV and $m_{\tilde{q}} = 50$ GeV; assuming $\lambda_{\bar{u}\bar{d}\bar{d}} = 1$. For larger gluino masses, one can put tighter cuts on the jet energies and reduce the background considerably. Therefore, the signal is larger than the background for some combinations of couplings and masses, and it also can be enhanced considerably by looking at the mass distribution of the jets: the QCD four jets are produced relatively uncorrelated, while the tri-jet mass distribution of the signal should peak around the gluino mass. Although the analysis is harder in this case than the two-jet mass distribution, the signal to noise ratio is much larger. Such jet spectroscopy is a challenge; frequently one of the three jets will be too soft to be measured as such and at other times jet coalescence would occur, especially for small values of the gluino mass.

Leptonic Decays

If the singly produced superpartner is not the LSP, it could first decay into the LSP via the usual gauge couplings. For example, $\tilde{\ell} \to \ell\tilde{\gamma}$ could dominate $\tilde{\ell} \to \bar{q}_i q_j$, where the photino would decay into a lepton and a pair of quarks. These events produce a striking signal. The topology of the event consists of an isolated lepton in one hemisphere balanced by a lepton plus two jets in the other hemisphere with no missing energy. This signature, with two leptons and two jets in the final state, is easier to see than a bump in the invariant mass plot. In fact, the background for this process is negligible. The standard model background arises from the production and decay of one Z^o plus two jets: $Z^o(\to \ell^+\ell^-) + two\ jets$. The cross section times the branching ratio is of the order of $10^{-3}nb$ (3) and can be greatly reduced by excluding lepton pairs with an invariant mass equal to the Z^o mass. Another source of background could be the Drell-Yan mechanism producing two leptons, accompanied by two jets. This process is suppressed by a factor $\frac{\alpha_e^2 \times \alpha_s^2}{\alpha_\lambda} \simeq \frac{10^{-6}}{\alpha_\lambda}$, compared to the single production of sleptons. This is not a severe background. Moreover, the signal can be enhanced greatly by looking at the invariant mass of the two jets and the lepton in the same hemisphere, which should peak around the photino mass. We therefore conclude that in the absence of any significant background, a minimum of 30 such events should constitute a clear signal for the production of the slepton. We have made no attempt to calculate the detector's efficiency for such events and feel that 30 is a conservative number. Figure 24 shows the slepton masses and the values for the couplings of the $q\bar{d}\ell$ operator, for which at least 30 sleptons will be produced at the Tevatron for the total integrated luminosity of $10pb^{-1}$. We emphasize again that if such leptonic decays do exist, Tevatron data will allow a search for single superparticle production over a considerable range of masses and for values of λ down to 10^{-2}.

For yet smaller values of the coupling constants ($\lambda < 10^{-2}$), the only observable evidence for superparticle decay in hadron colliders would be squark or gluino pair production and the subsequent decay of the LSP due to the B- and L-number violating operators. In the next subsection we are going to discuss some of the

signatures arising from the pair production of superparticles. We shall see that there is a wealth of interesting possibilities.

b) Superparticle Pair Production and Decay

For small $\lambda(\lambda \lesssim 10^{-2})$, the dominant production mechanism for the superpartners is the pair production of squarks and gluinos via the usual gauge couplings. If the pair produced superparticle is the LSP, it will decay via the B- or L-number violating interactions. If it is not the LSP, it will first decay into the LSP, and then the LSP will decay. In Table 1, we enumerate various candidates for the LSP and their decay modes in the presence of any of the Yukawa interactions. We must stress again the significance of leptons in the final states. The majority of events with singly or doubly produced superpartners can contain single isolated leptons. For example, if squark is the LSP decaying via the $q\bar{d}\ell$ operator, the signal consists of two jets and two leptons, with the invariant mass of the jet–lepton system strongly peaked around the squark mass. We have already mentioned that the background for such events is very small, making these leptonic decays the best signatures to look for.

The production cross sections for gluino pairs and squark pairs are relatively large (Figs. 14 and 16). For example, the gluino pair production is about $0.3nb$ at Tevatron energies, for $m_{\tilde{g}} = m_{\tilde{q}} = 100$ GeV, which means about $3,000$ such pairs can be produced with an integrated total luminosity of $10pb^{-1}$. With such a large rate of production, the prospects of detecting superparticles through their B- and L-number violating decays are enormous.

4.3. Searches for Gaps, Secondary Vertices and Stable Particles

In the previous sections we assumed that the strength of the Yukawa couplings are large ($\lambda \gtrsim 10^{-2}$). All the results can be rescaled for new λ's if this is not the case. However, a small coupling means that perhaps the LSP is long lived, which suggests a new set of possibilities for accelerator signatures. The LSP can travel a

macroscopic distance and decay inside or outside the detector; and if charged, it can leave a track. For example, assume the squark is the LSP. Its lifetime is

$$\tau_{\tilde{q}} = 10^{-9} sec \times (\frac{100GeV}{m_{\tilde{q}}})(\frac{10^{-8}}{\lambda})^2.$$

For $\lambda \lesssim 10^{-8}$, a squark, after being pair produced, can either decay in the tracking chambers leaving a secondary vertex, or may be stopped in the hadronic calorimeter and produce hadronic showers when it decays. If the LSP is neutral, there would be a gap between the primary and the secondary vertices. Such events are so prominent that only a few would constitute a clean signal. This gives sensitivity to smaller couplings all the way down to 10^{-10} for the sneutrinos; the small fraction of sneutrinos which decay in the detector before escaping would be sufficient to give a signal. Larger couplings, $\lambda \sim 10^{-7}$ for a 100 GeV superpartner, could be probed in future runs with a vertex detector.

CONCLUSION

To summarize, we have stressed the possibility that the LSP can decay even in supersymmetric models with the minimal field content. We have presented the production cross sections for supersymmetric particles from B- and L-violating Yukawa couplings. We were able to set some limits on the strength of these couplings and the masses of some superpartners using existing data from the CERN collider. We discussed the prospects for detecting these processes at the Fermilab Tevatron, and find that a run of $10pb^{-1}$ will enable a large new region of the parameter space to be explored.

Acknowledgements:

S.D. acknowledges support by the National Science Foundation under Grant NSF–PHY–86–12280 to Stanford University. G.D.S. is funded by NSF under grant PHY86–20266 and a fellowship from the W. H. Keck Foundation. R.E. acknowledges support by the Department of Energy, contract DE–AC03–76SF00515 at Stanford Linear Accelerator Center. L.J.H. acknowledges support by the Director,

Office of Energy Resources, Office of High Energy and Nuclear Physics, Division of High Energy of the U. S. Dept. of Energy under contract DE–AC03–7600098, and in part by NSF under Grant PHY–85–15857. L.J.H. also acknowledges partial support by a Sloan Foundation Fellowship and a Presidential Young Investigator Award.

TABLE 1

In this table, q represents a quark or an antiquark, and ℓ could be a lepton of any charge.

LSP	$\bar{u}\bar{d}\bar{d}$	$q\bar{d}\ell$	$\ell\ell\bar{e}$
Charged, Strongly Interacting	$\tilde{q} \to qq$	$\tilde{q} \to q\ell$	$\tilde{q} \to q\ell\ell\ell$
Neutral, Strongly Interacting	$\tilde{g} \to qqq$	$\tilde{g} \to qq\ell$	$\tilde{g} \to qq\ell\ell\ell$
Charged, Weakly Interacting	$\tilde{\ell}^{\pm} \to \ell qqq$	$\tilde{\ell}^{\pm} \to q\ell$	$\tilde{\ell}^{\pm} \to \ell\ell$
Neutral, Weakly Interacting	$\tilde{\nu} \to \ell qqq$	$\tilde{\nu} \to q\ell$	$\tilde{\nu} \to \ell\ell$
	$\tilde{\gamma} or \tilde{Z} \to qqq$	$\tilde{\gamma} or \tilde{Z} \to \ell qq$	$\tilde{\gamma} or \tilde{Z} \to \ell\ell\ell$

FIGURE CAPTIONS

1) Yukawa interactions resulting from operators from Eqs. (1.1) and (1.2). Solid lines are fermions and dashed lines are scalars. Tilde denotes a superpartner. There are two more interactions for each operator obtained by permuting the position of each superpartner. Particles could be of any flavor.

2) The parton diagram for single sneutrino production.

3) Quantity $(\tau/\hat{s}\frac{d\mathcal{L}}{d\tau})$ for $d-\bar{d}$ interactions in proton–antiproton collisions. Collider energies $\sqrt{s}$ are given in TeV.

4) Total cross section for $p\bar{p} \to \tilde{\nu}$, with $\tilde{\nu}$ masses of 50, 100 and 250 GeV, for $\lambda_{q\bar{d}\ell} = 1$.

5) Quantity $(\tau/\hat{s}\frac{d\mathcal{L}}{d\tau})$ for $u-\bar{d}$ and $\bar{u}-d$ interactions in proton–antiproton collisions.

6) Total cross section for $p\bar{p} \to \tilde{\ell}^{\pm}$, with $\tilde{\ell}^{\pm}$ masses of 20, 50, 100 and 250 GeV, for $\lambda_{q\bar{d}\ell} = 1$.

7) The parton diagram for single squark production.

8) Quantity $\tau/\hat{s}\frac{d\mathcal{L}}{d\tau}$ for $u-d$ and $\bar{u}-\bar{d}$ interactions in proton–antiproton collisions.

9) Total cross section for $p\bar{p} \to \tilde{q}^{\pm 1/3}$, with $\tilde{q}^{\pm 1/3}$ masses of 20, 50, 100 and 250 GeV, with $\lambda_{\bar{u}\bar{d}\bar{d}} = 1$.

10) Feynman diagrams for single gluino production in quark–quark scattering.

11) Total cross section $p\bar{p} \to \tilde{g}q$, for gluino and squark masses 50, 50; 100, 100; and 250, 250 GeV.

12) Production and decay of a single gluino, if the dominant operator is $\bar{c}\bar{b}\bar{s}$.

13) Total cross section $p\bar{p} \to \tilde{g}q$, if the dominant "$\Delta B \neq 0$" operator is $\bar{c}\bar{b}\bar{s}$, for gluino and squark masses 50, 50; 100, 100; and 250, 250 GeV.

14) Total cross section for $p\bar{p} \to \tilde{g}\tilde{g}$. The masses of the gluinos and the squarks are 3, 20; 50, 50; and 100, 100 GeV. The plot is reproduced from Ref. (4).

15) The total cross section for slepton pair production, for slepton masses of 20, 50, 100 and 250 GeV, for $\lambda = 1$.

16) Total cross section for production of two squarks via the standard gauge couplings. The cross section is the same for an antisquark pair or a squark–antisquark pair. All masses are as in Fig. 14. The plot is reproduced from Ref. (4).

17) Total cross section for production of two squarks (or antisquarks, or a squark–antisquark pair) via the $\bar{u}\bar{d}\bar{d}$ operator. All masses are as in Fig. 9.

18) Upper limits on the cross section times decay branching ratio for the production of a particle X decaying into two hadronic jets, shown as a function of mass M_X. The limits are shown for $\Gamma_X < 0.4 M_X$. The broken lines show our predictions for the production of sneutrinos, squark and sleptons at the CERN collider ($\sqrt{s} = 630$ GeV), for $\lambda = 2.2$.

19) The jet-pair mass distribution, for invariant masses between 45 and 175 GeV. Figure is taken from Ref. (16).

20) Upper limits on the cross section times decay branching ratio for the production of a particle X decaying into two hadronic jets, shown as a function of mass M_X, derived from the UA2 published results (Ref. (16)). The limits are shown for $\Gamma_X < 0.1 M_X$. The broken lines show our predictions for the production of sneutrinos, squark and sleptons at the CERN collider ($\sqrt{s} = 630$ GeV), for $\lambda = 1.3$.

21) The excluded region of parameter space for single slepton, squark and sneutrino production, using the UA1 and UA2 data. The dark region is excluded by our analysis, and we expect the shaded region to be excluded by a more detailed Monte Carlo simulation.

22) Invariant mass spectrum for two-jet events produced in proton–antiproton

collisions at $\sqrt{s} = 2$ TeV. Both jets must satisfy the rapidity cut $|y| < 0.85$. The dashed line shows the peak of the signal for sneutrino decay into two jets.

23) The total integrated luminosity necessary to discover a sneutrino for $\sqrt{s} =$ 2 TeV, in the $q\bar{d}\ell$ model for $\lambda = 1$.

24) For these slepton masses and couplings ($\lambda_{q\bar{d}\ell}$), at least 30 sleptons are going to be produced at the c.m. energy of 2 TeV at the Fermilab Tevatron, for a total integrated luminosity of $10pb^{-1}$.

REFERENCES

1. H. E. Haber and G. L. Kane, Phys. Rev., **117** (1985) p. 75.
2. S. Dimopoulos and L. J. Hall, Phys. Lett., B **207** (1988) p. 210.
3. E. Eichten, I. Hinchliffe, K. Lane and C. Quigg, Rev. Mod. Phys., **56** (1984) p. 579.
4. S. Dawson, E. Eichten and C. Quigg, Phys. Rev., D **31** (1985) p. 1581.
5. L. J. Hall and M. Suzuki, Nucl. Phys., B **231** (1984) p. 419.
6. C. Aulakh and R. Mohapatra, Phys. Lett., B **119** (1983) p. 136.
7. I. H. Lee, Nucl. Phys., B **246** (1984) p. 120.
8. G. G. Ross and J. W. F. Valle, Phys. Lett., B **151** (1985) p. 375.
9. J. Ellis, G. Gelmini, C. Jarlskog, G. G. Ross and J. W. F. Valle, Phys. Lett., B **150** (1985) p. 142.
10. S. Dawson, Nucl. Phys., B **261** (1985) p. 297.
11. F. Zwirner, Phys. Lett., B **132** (1983) p. 103.
12. R. Barbieri and A. Masiero, Nucl. Phys., B **267** (1986) p. 679.
13. S. Dimopoulos and L. J. Hall, Phys. Lett., B **135** (1987) p. 135.
14. C. Quigg, *Gauge Interactions of the Strong, Weak, and Electromagnetic Interactions* (Benjamin-Cummings, Mass., 1983).
15. C. Albajar et al, Phys. Lett., B **209** (1988) p. 127.
16. R. Ansari et al, Phys. Lett., B **186** (1987) p. 452.
17. G. Altarelli et al., Nucl.Phys., B **246** (1984) p. 12; Z. Phys. C, **27** (1985) p. 617.
18. E. N. Argyres, C. G. Papadopoulos and S. D. P. Vlassopoulos, Phys. Lett., B **202** (1988) p. 425.

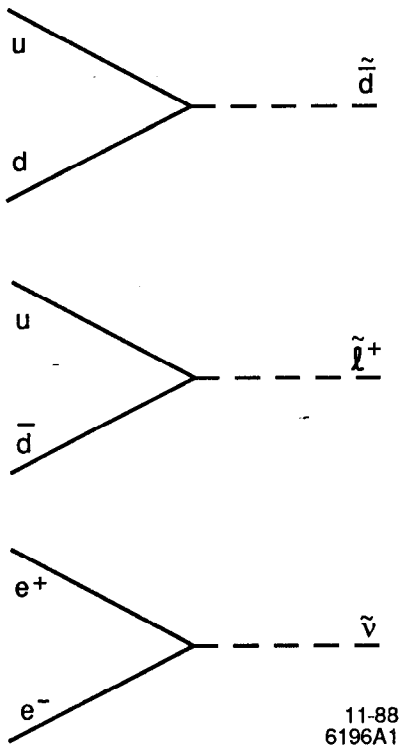

Fig. 1

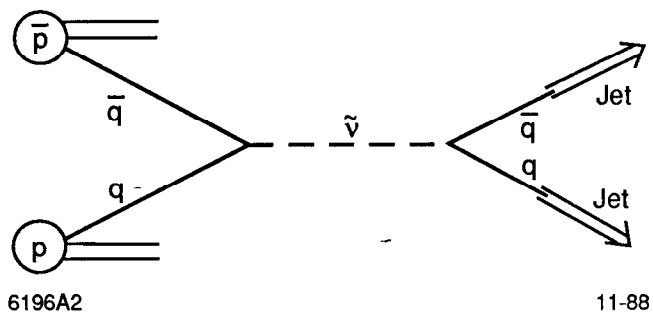

Fig. 2

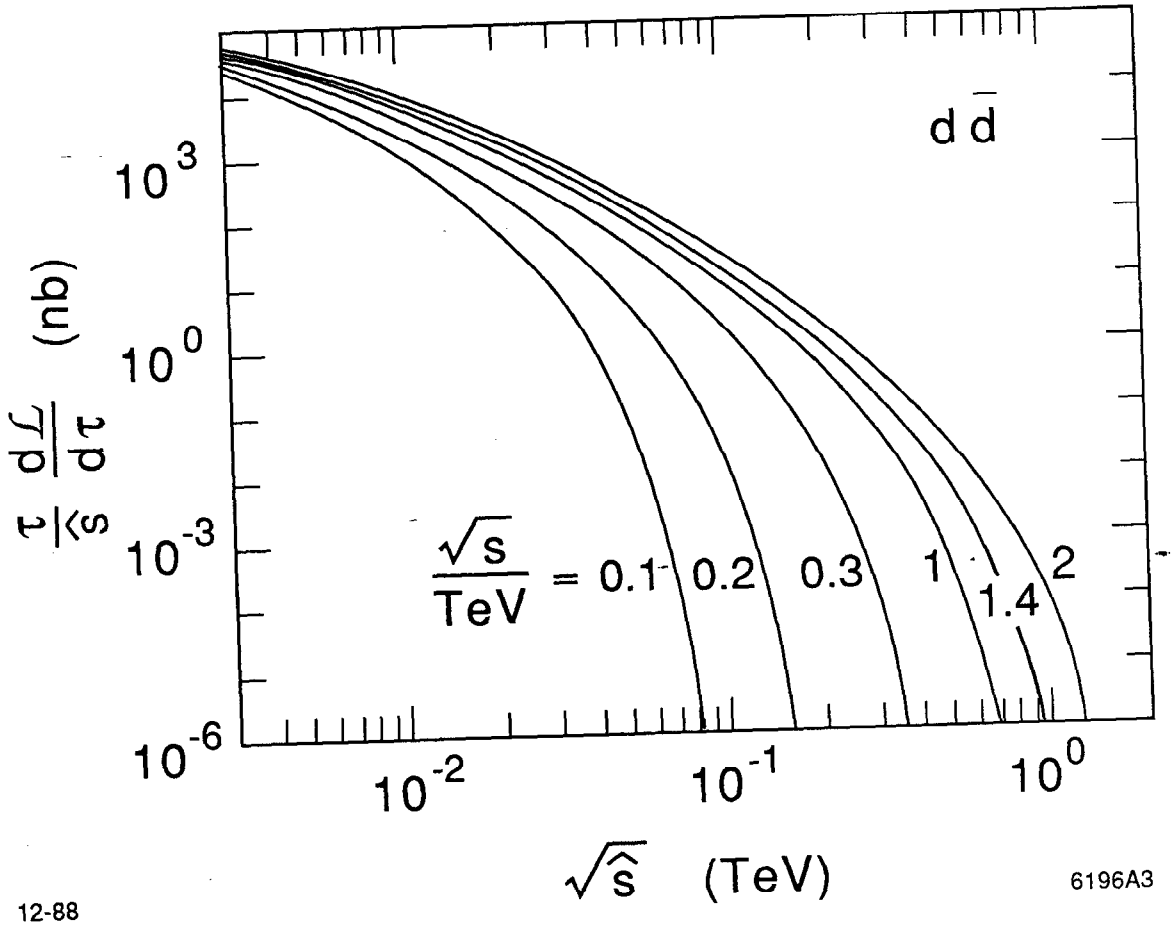
d d̄
10^3
10^0
10^{-3}
10^{-6}
$\tau \frac{d\mathcal{L}}{d\tau}\Big|_{\langle s \rangle}$ (nb)
$\frac{\sqrt{s}}{\text{TeV}}$ = 0.1
0.2
0.3
1
1.4
2
10^{-2}
10^{-1}
10^0
$\sqrt{\hat{s}}$ (TeV)
6196A3

12-88

Fig. 3

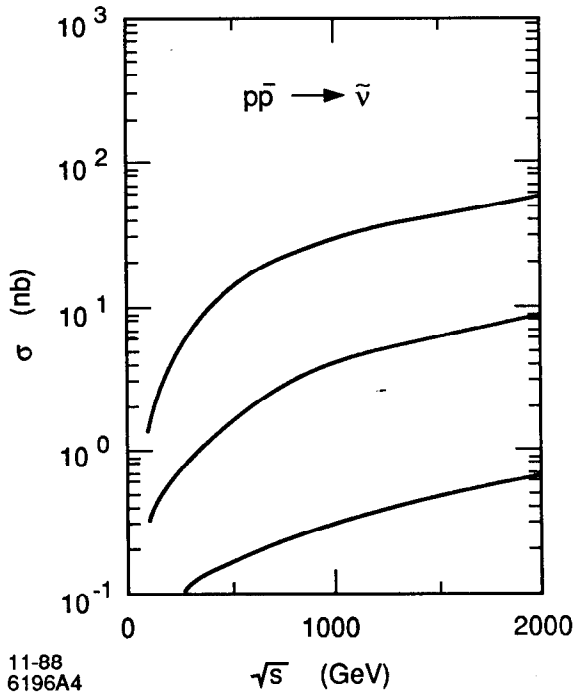
10^3
10^2
10^1
10^0
10^{-1}
$p\bar{p} \rightarrow \tilde{\nu}$
σ (nb)
0
1000
2000
$\sqrt{s}$ (GeV)
11-88
6196A4

Fig. 4

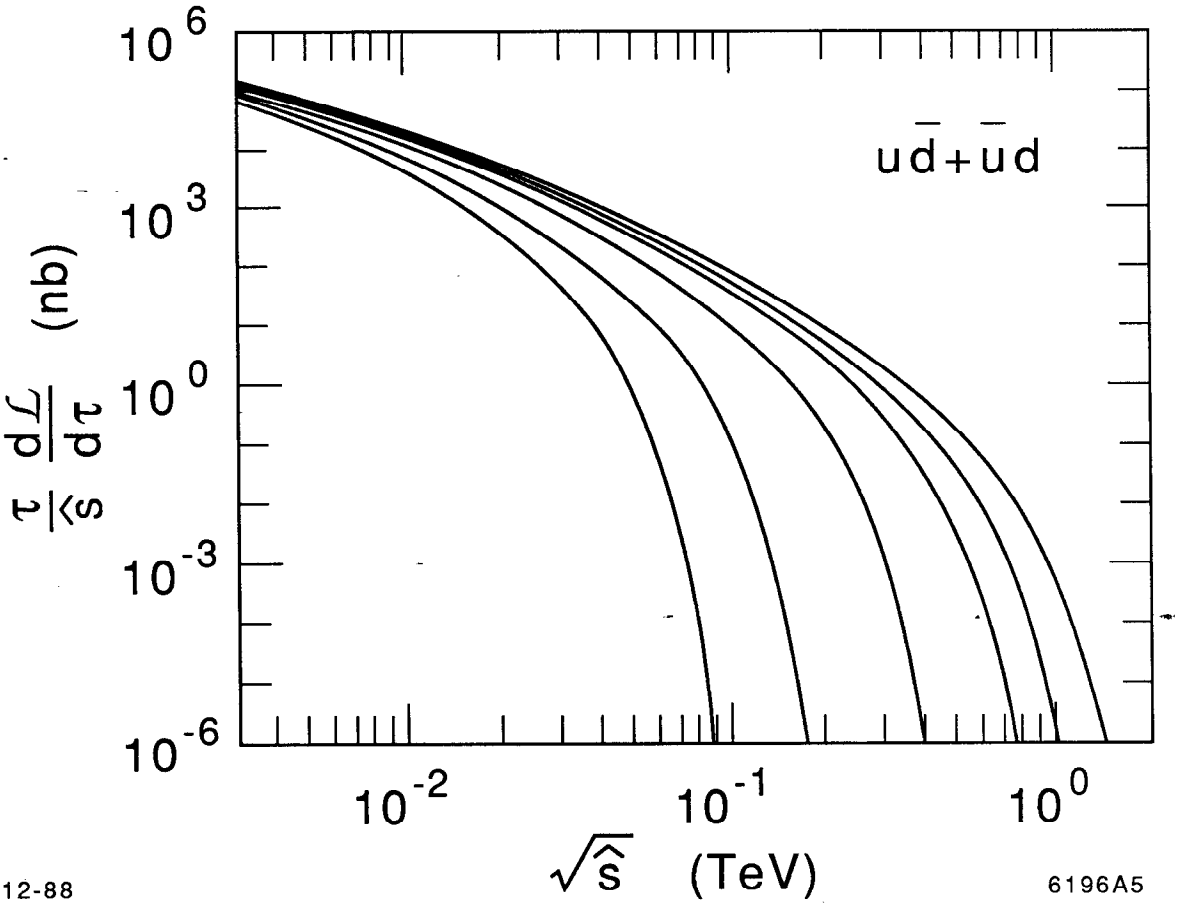
10^6
10^3
10^0
10^{-3}
10^{-6}
$\tau \left| \frac{d\mathcal{L}}{d\tau} \right|_{\hat{s}}$ (nb)
$u\bar{d}+\bar{u}d$
10^{-2}
10^{-1}
10^0
$\sqrt{\hat{s}}$ (TeV)
12-88
6196A5

Fig. 5

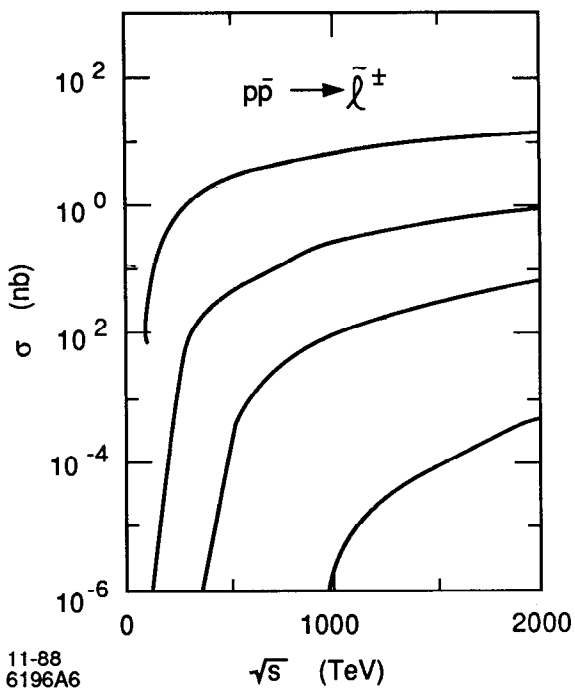
$p\bar{p} \rightarrow \tilde{\ell}^{\pm}$
10^{2}
10^{0}
10^{2}
10^{-4}
10^{-6}
σ (nb)
0
1000
2000
$\sqrt{s}$ (TeV)
11-88
6196A6

Fig. 6

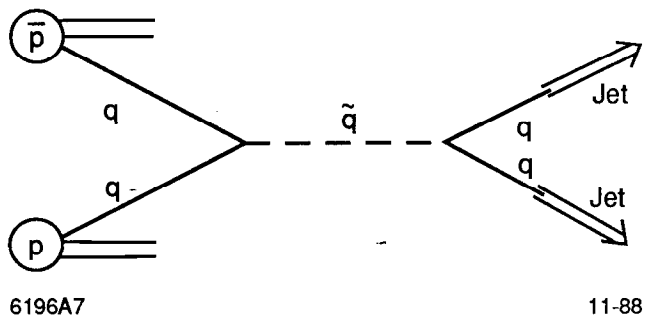

Fig. 7

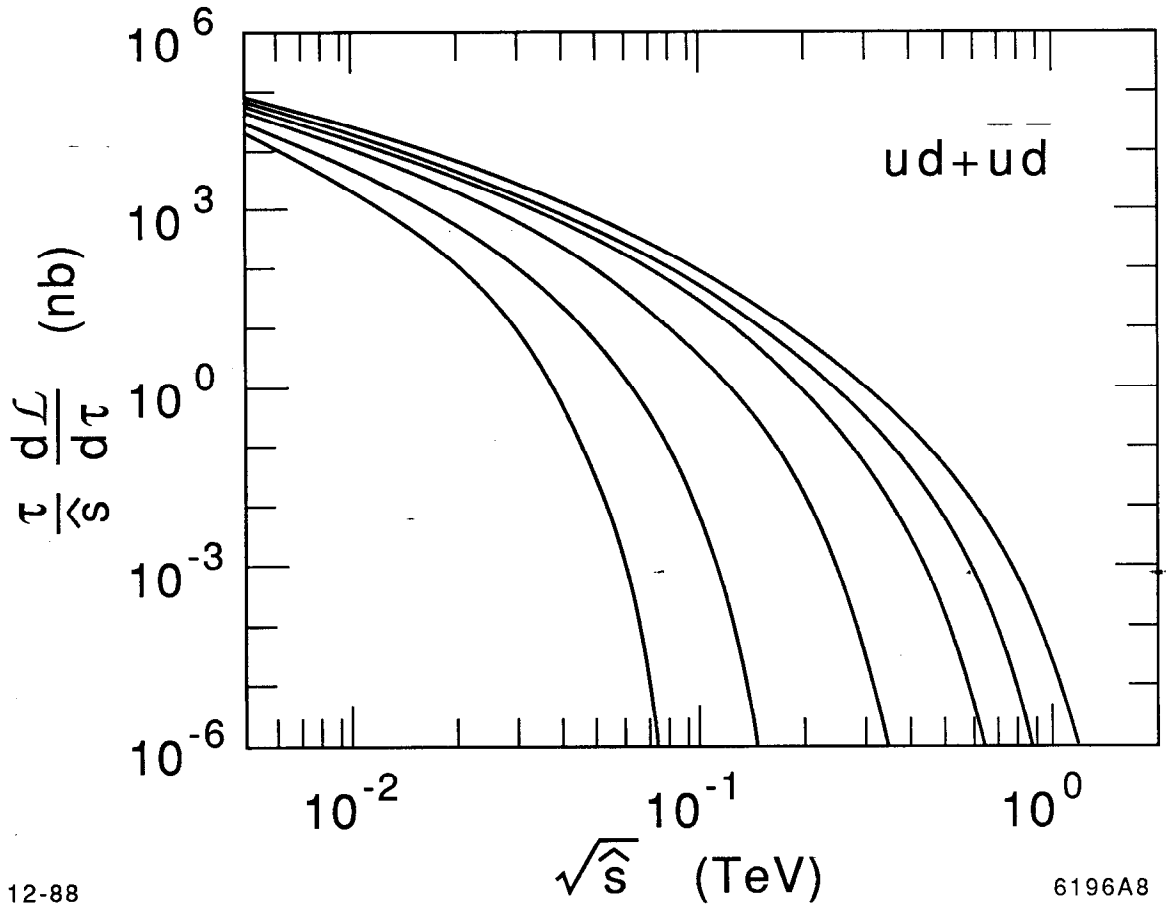
10^6
10^3
10^0
10^{-3}
10^{-6}
$\tau \frac{d\mathcal{L}}{d\tau} \langle s \rangle$ (nb)
$ud+\bar{u}\bar{d}$
10^{-2}
10^{-1}
10^0
$\sqrt{\hat{s}}$ (TeV)
12-88
6196A8

Fig. 8

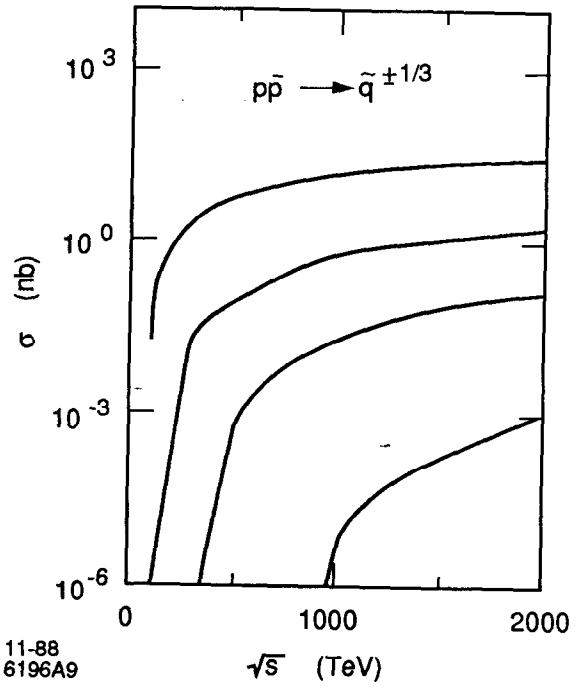
$p\bar{p} \rightarrow \tilde{q}^{\pm 1/3}$
10^{3}
10^{0}
10^{-3}
10^{-6}
σ (nb)
0
1000
2000
$\sqrt{s}$ (TeV)
11-88
6196A9

Fig 9

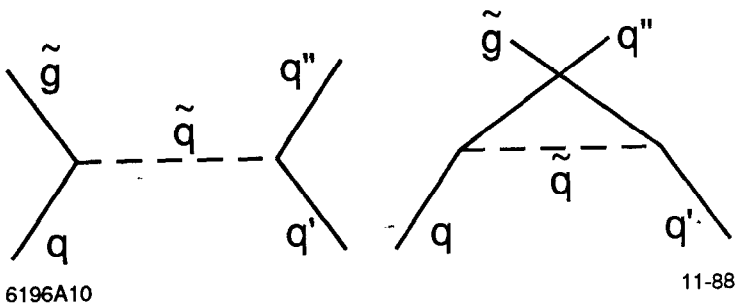

Fig. 10

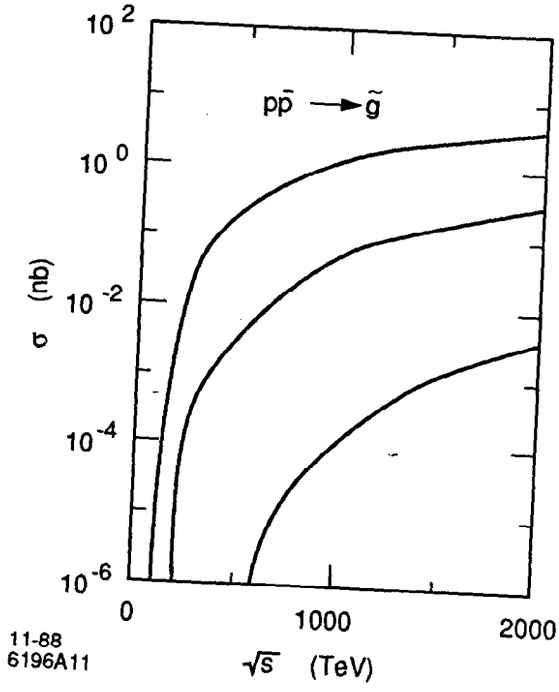
10^2
10^0
10^{-2}
10^{-4}
10^{-6}
σ (nb)
$p\bar{p} \rightarrow \tilde{g}$
0
1000
2000
$\sqrt{s}$ (TeV)
11-88
6196A11

Fig. 11

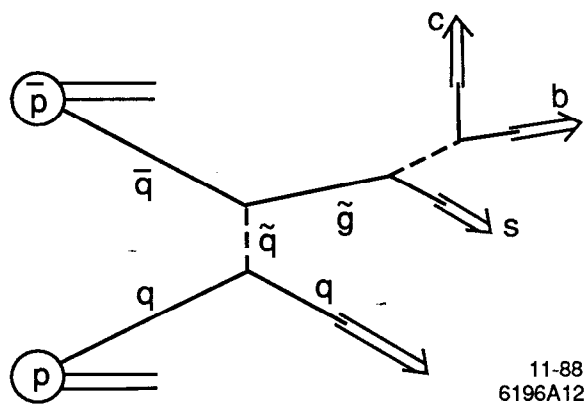

Fig. 12

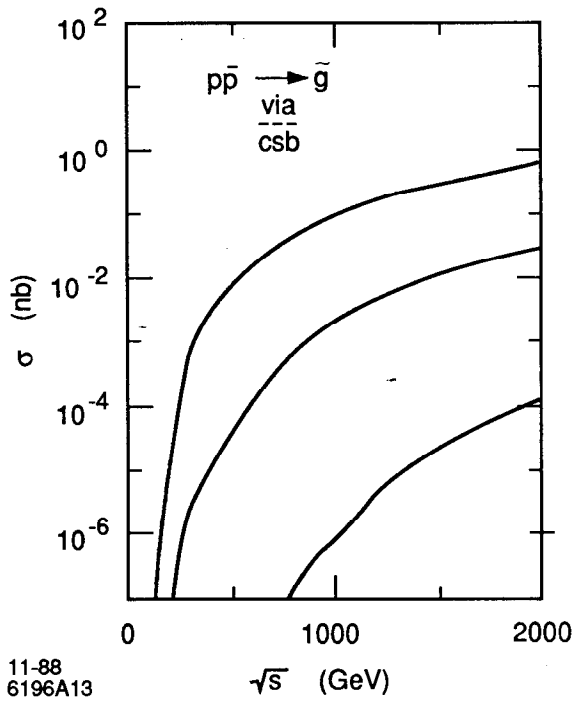
10^2
10^0
10^{-2}
10^{-4}
10^{-6}
σ (nb)
$p\bar{p} \longrightarrow \tilde{g}$
via
$\overline{csb}$
0
1000
2000
$\sqrt{s}$ (GeV)
11-88
6196A13

Fig. 13

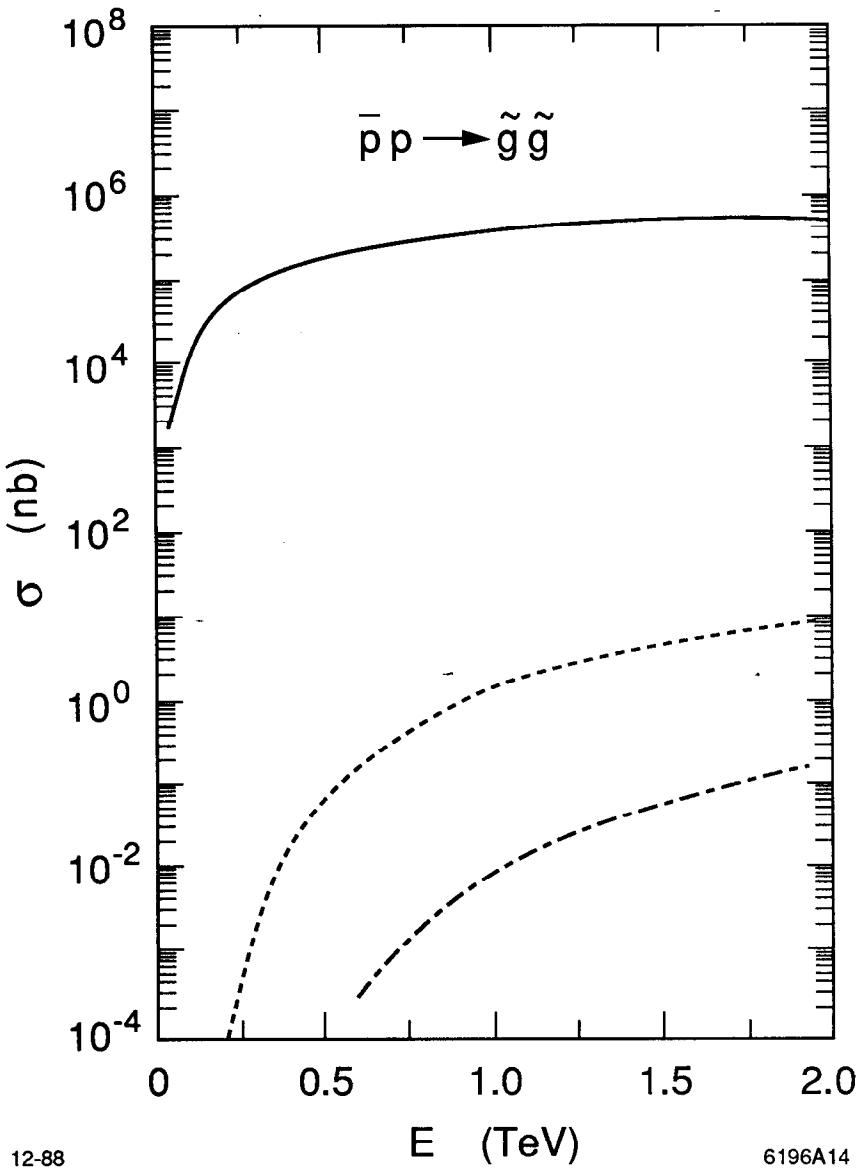
$\bar{p}p \rightarrow \tilde{g}\tilde{g}$
10^8
10^6
10^4
10^2
10^0
10^{-2}
10^{-4}
σ (nb)
0
0.5
1.0
1.5
2.0
E (TeV)
12-88
6196A14

Fig. 14

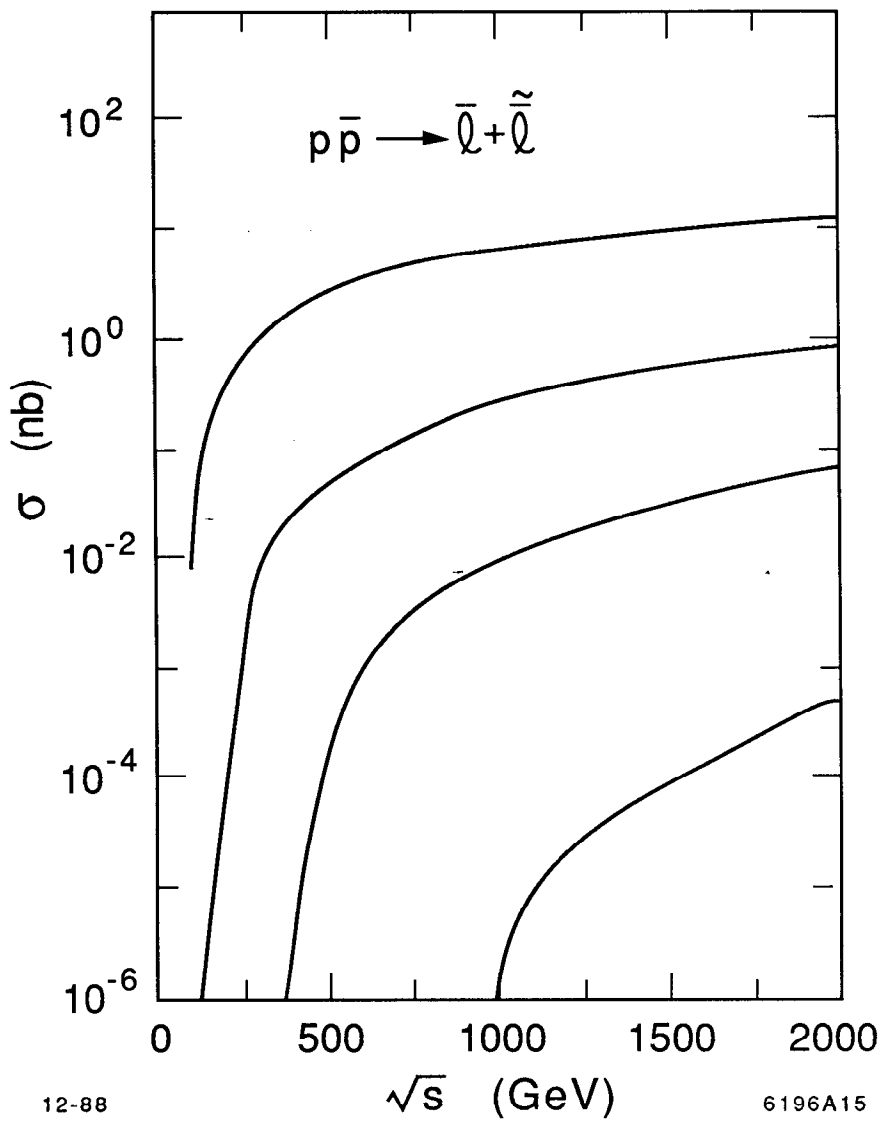
$p\bar{p} \longrightarrow \bar{\ell}+\tilde{\bar{\ell}}$
10^2
10^0
10^{-2}
10^{-4}
10^{-6}
σ (nb)
0
500
1000
1500
2000
$\sqrt{s}$ (GeV)
12-88
6196A15

Fig. 15

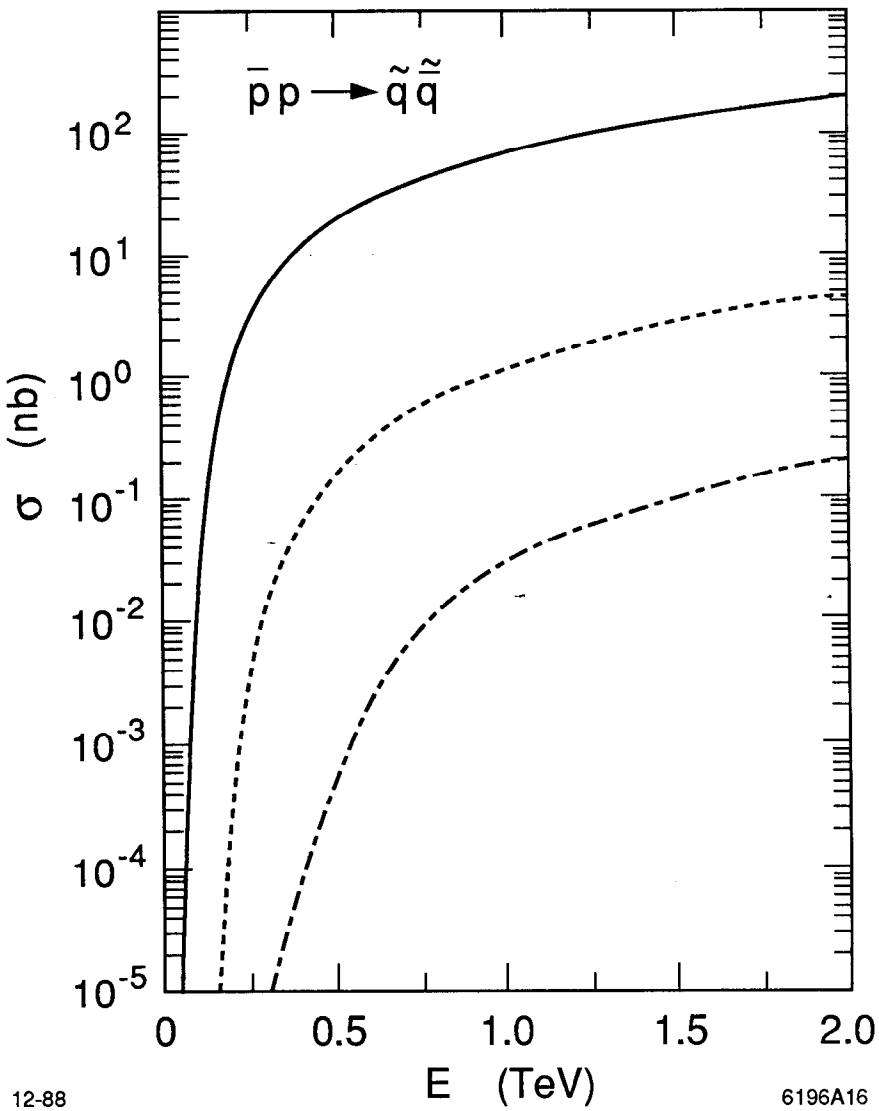
$\bar{p}p \rightarrow \tilde{q}\bar{\tilde{q}}$
10^2
10^1
10^0
10^{-1}
10^{-2}
10^{-3}
10^{-4}
10^{-5}
σ (nb)
0
0.5
1.0
1.5
2.0
E (TeV)
12-88
6196A16

Fig. 16

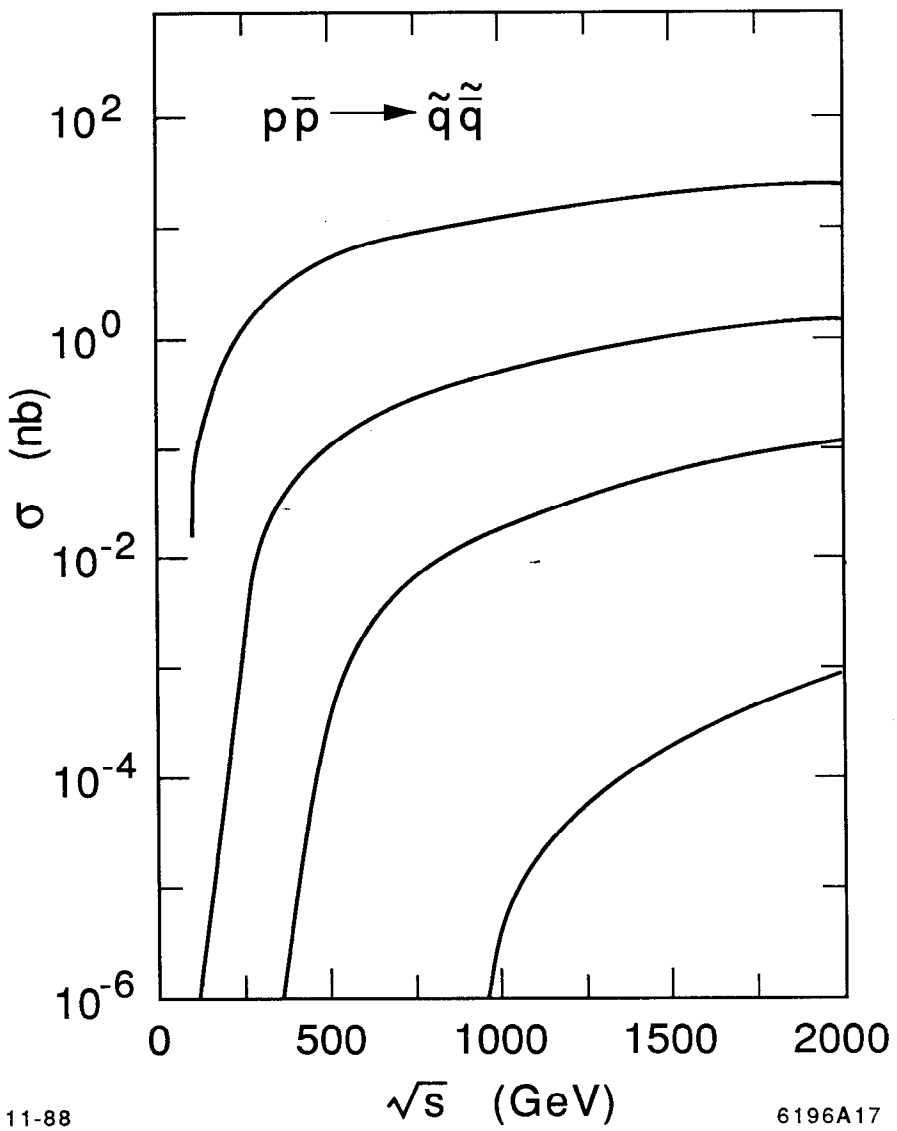
$p\bar{p} \rightarrow \tilde{q}\bar{\tilde{q}}$
10^2
10^0
10^{-2}
10^{-4}
10^{-6}
σ (nb)
0
500
1000
1500
2000
$\sqrt{s}$ (GeV)
11-88
6196A17

Fig. 17

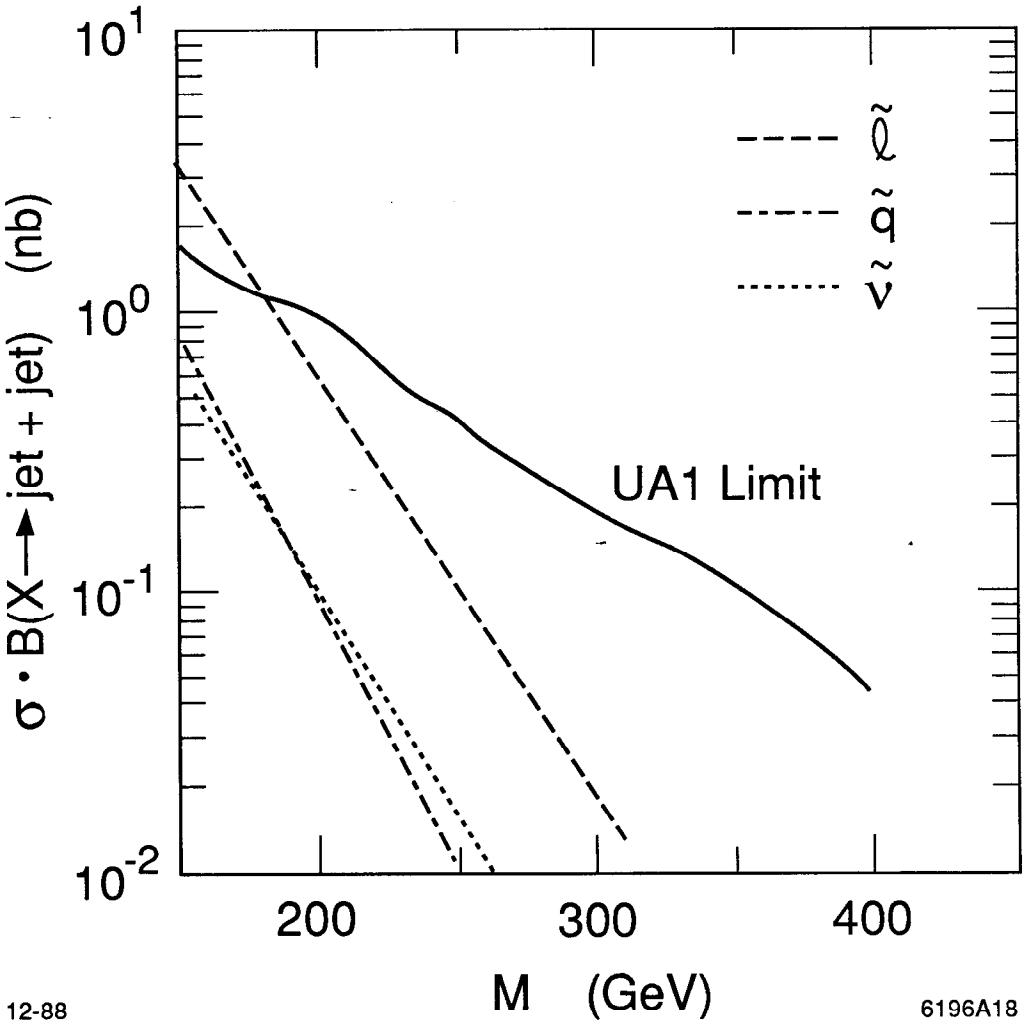
10^1
10^0
10^{-1}
10^{-2}
$\sigma \cdot B(X \rightarrow \text{jet} + \text{jet})$ (nb)
200
300
400
M (GeV)
$\tilde{\ell}$
$\tilde{q}$
$\tilde{\nu}$
UA1 Limit
12-88
6196A18

Fig. 18

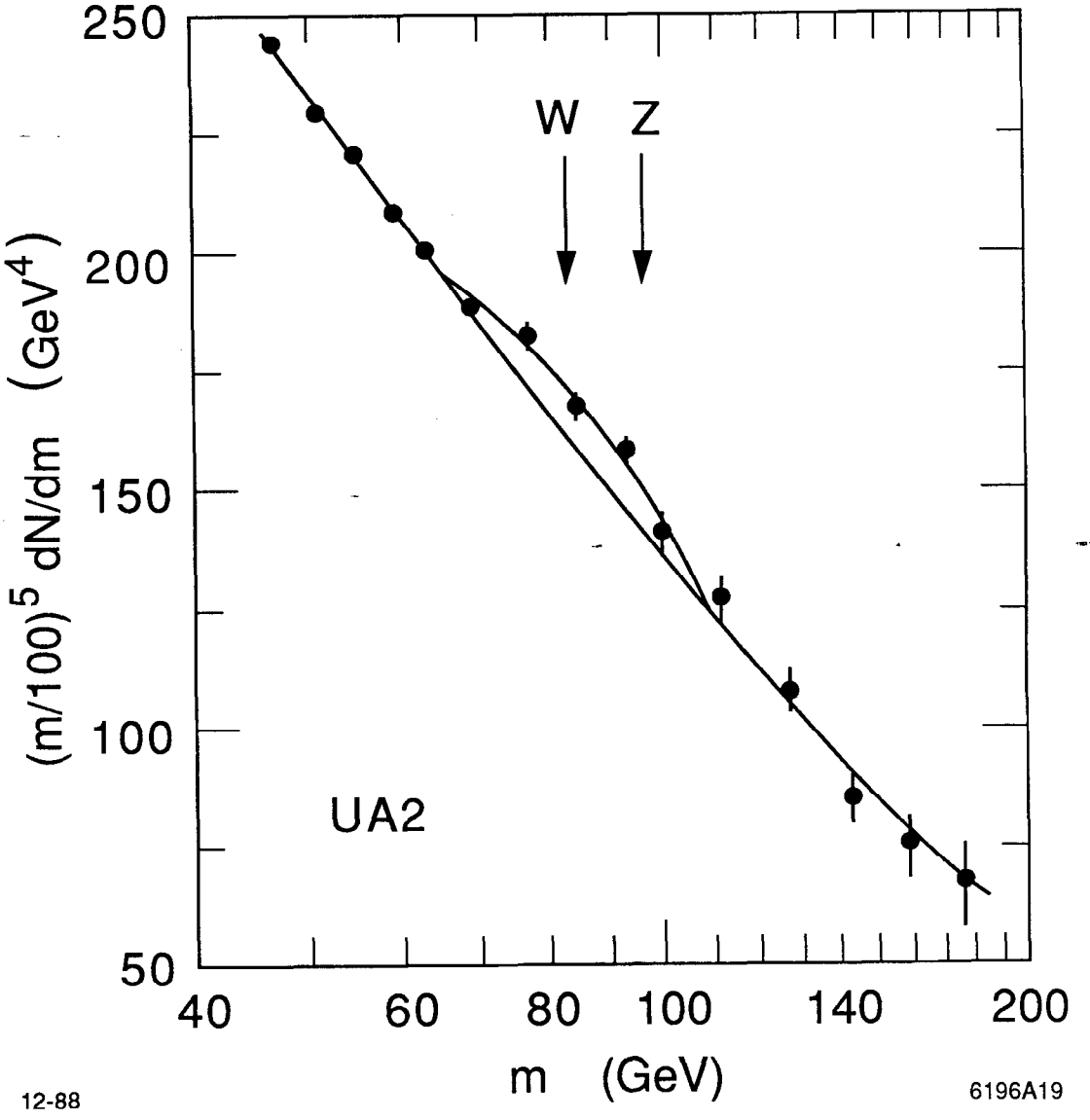
250
200
150
100
50
40
60
80
100
140
200
W
Z
UA2
$(m/100)^5$ dN/dm (GeV^4)
m (GeV)
12-88
6196A19

Fig. 19

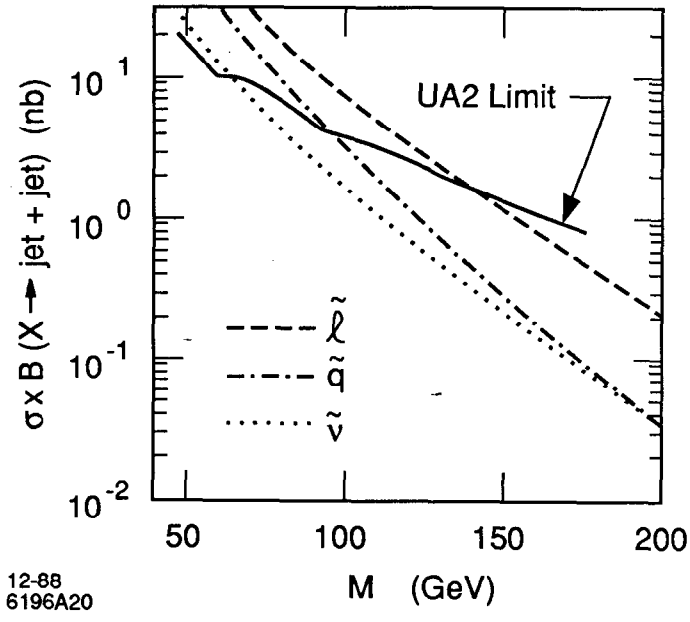
UA2 Limit
$\tilde{\ell}$
$\tilde{q}$
$\tilde{\nu}$
$\sigma \times B\ (X \rightarrow \text{jet} + \text{jet})$ (nb)
10^{1}
10^{0}
10^{-1}
10^{-2}
50
100
150
200
M (GeV)
12-88
6196A20

Fig. 20

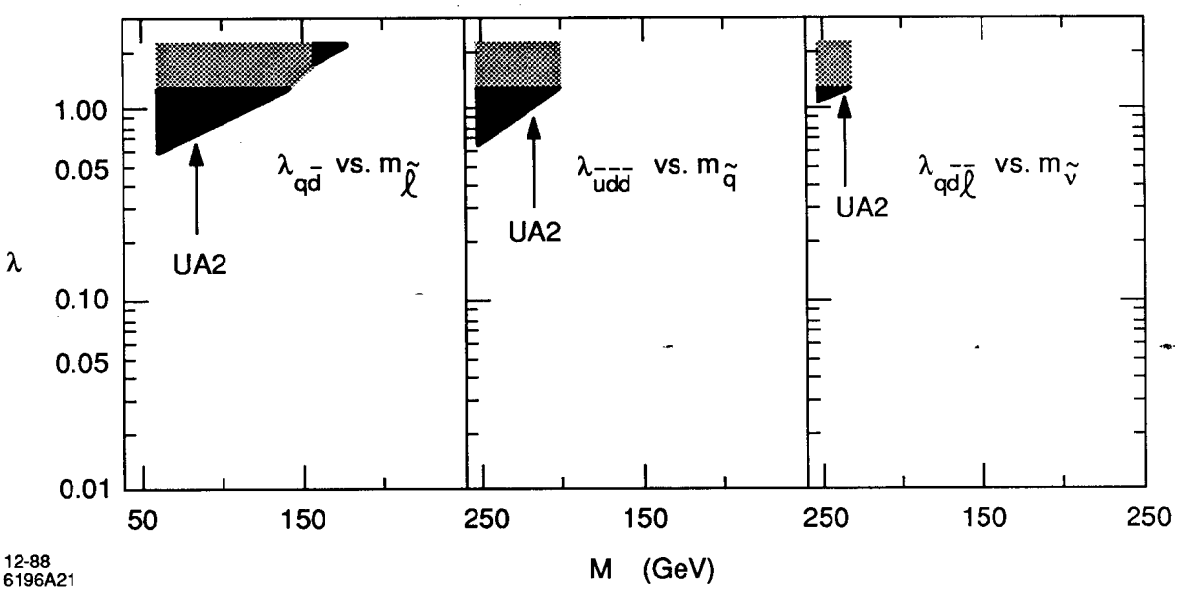
1.00
0.05
λ
0.10
0.05
0.01
UA2
$\lambda_{q\bar{d}}$ vs. $m_{\tilde{\ell}}$
UA2
$\lambda_{\bar{u}\bar{d}\bar{d}}$ vs. $m_{\tilde{q}}$
UA2
$\lambda_{q\bar{d}\bar{\ell}}$ vs. $m_{\tilde{\nu}}$
50
150
250
150
250
150
250
M (GeV)
12-88
6196A21

Fig. 21

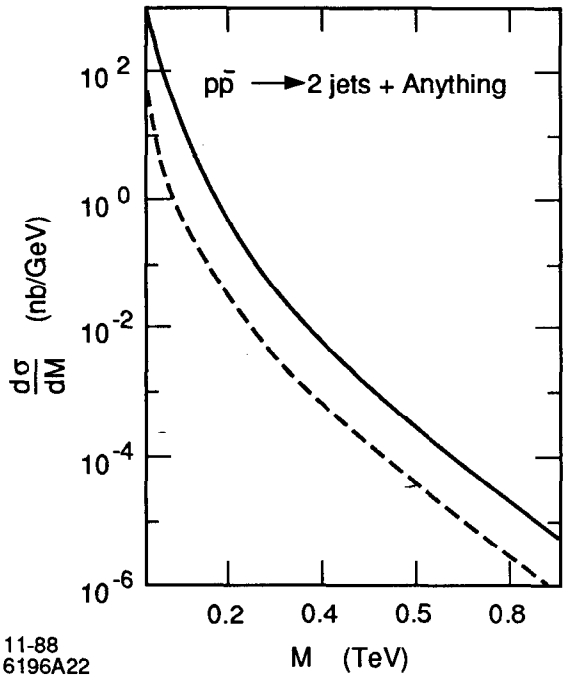
$p\bar{p} \longrightarrow$ 2 jets + Anything
10^{2}
10^{0}
10^{-2}
10^{-4}
10^{-6}
$\frac{d\sigma}{dM}$ (nb/GeV)
0.2
0.4
0.5
0.8
M (TeV)
11-88
6196A22

Fig. 22

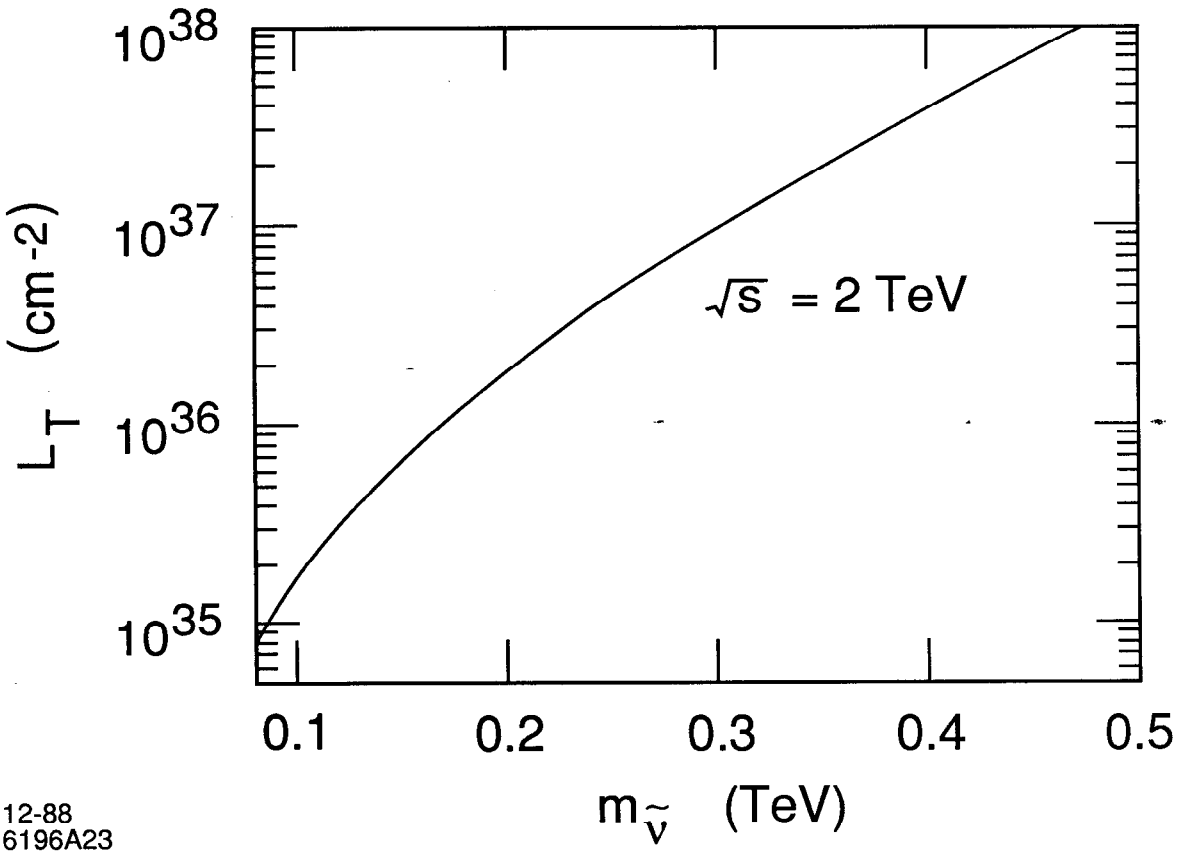

12-88
6196A23

Fig. 23

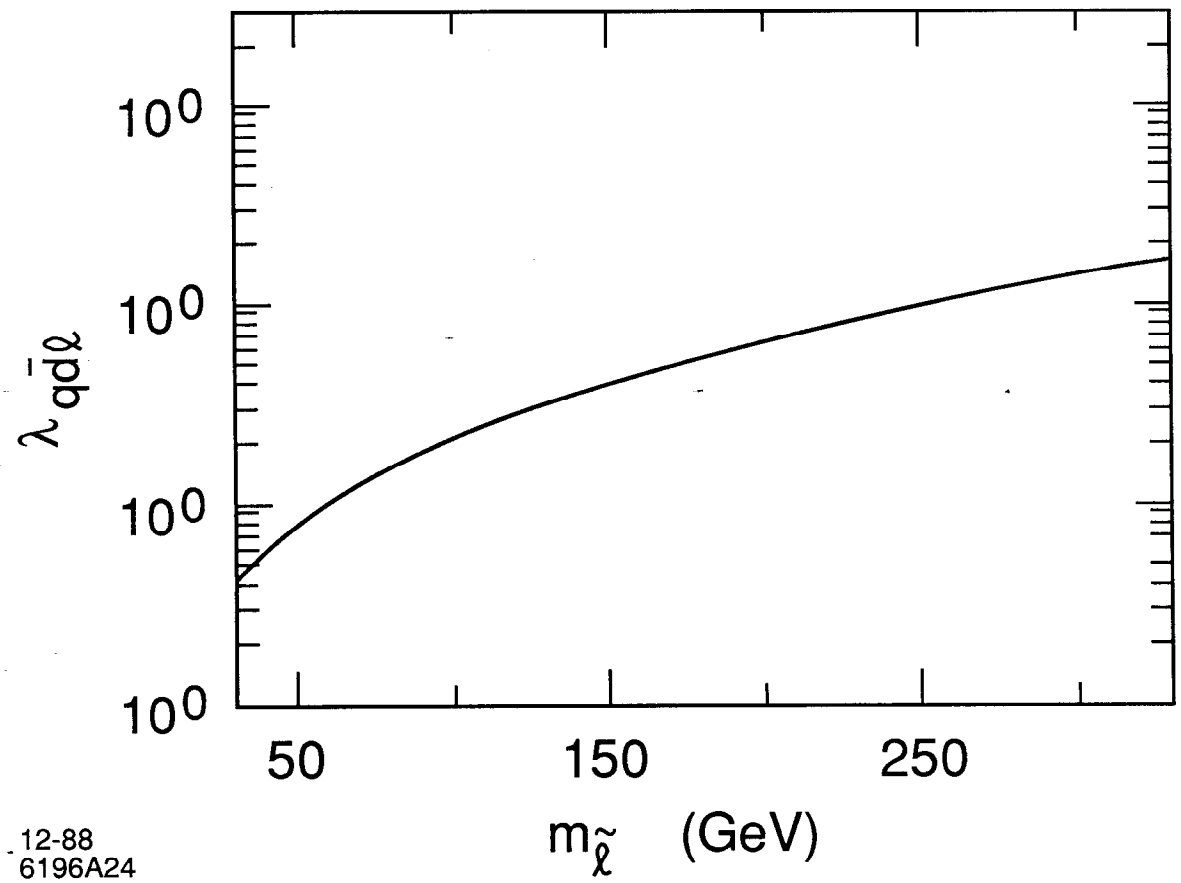

12-88
6196A24

Fig. 24